

Published in final edited form as:

ACS Nano. 2009 August 25; 3(8): 2147–2152. doi:10.1021/nn9003814.

## Nano-Flares for mRNA Regulation and Detection

**Andrew E. Prigodich, Dwight S. Seferos, Matthew D. Massich, David A. Giljohann, Brandon C. Lane, and Chad A. Mirkin**

Department of Chemistry and International Institute for Nanotechnology, Northwestern University, 2145 Sheridan Road, Evanston, Illinois 60208-3113, USA

### Abstract

We build off the previously described concept of a nano-flare to develop an oligonucleotide gold nanoparticle conjugate that is capable of both detecting and regulating intracellular levels of mRNA. We characterize the binding rate and specificity of these materials using survivin, a gene associated with the diagnosis and treatment of cancer, as a target. The nanoconjugate enters cells and binds mRNA, thereby decreasing the relative abundance of mRNA in a dose- and sequence-dependent manner and resulting in a fluorescent response. This represents the first demonstration of a single material capable of both mRNA regulation and detection. Further, we investigate the intracellular biochemistry of the nanoconjugate, elucidating its mechanism of gene regulation. This work is important to the study of biologically active nanomaterials such as the nano-flare and is a first step towards the development of an mRNA responsive ‘theranostic’.

### Keywords

Nanoparticle; oligonucleotide; mRNA; detection; gene regulation; theranostic

Over the past decade, researchers have investigated the conjugation of biomolecules to inorganic nanomaterials, which has led to the development of hybrid materials with new activities.<sup>1–20</sup> One important class of hybrid nanomaterial is composed of a gold nanoparticle functionalized with a dense monolayer of oligonucleotides. These polyvalent nanoconjugates have many interesting properties, including distance-dependent optical features,<sup>21, 22</sup> enhanced nucleic acid binding,<sup>23</sup> resistance to degradation,<sup>24</sup> and the ability to enter cells without use of transfection agents.<sup>25</sup> These remarkable properties have enabled controlled assembly of materials,<sup>26–28</sup> molecular diagnostics,<sup>29–32</sup> and intracellular studies.<sup>33–35</sup>

Materials with both regulation and detection capabilities are of growing interest for use in personalized medicine.<sup>36</sup> These ‘theranostic’ materials have the potential to both treat and diagnose disease and are useful for investigating intracellular events (i.e. target recognition and control of biological function). Traditionally, antisense oligonucleotides and molecular beacons have been used to regulate and detect intracellular mRNA, respectively. Antisense oligonucleotides regulate gene expression by binding target mRNA and preventing translation.<sup>37</sup> Molecular beacons detect nucleic acids by coupling a binding event with a signal transduction mechanism, such as the separation of a fluorophore-quencher pair.<sup>38</sup> Given that cell entry and mRNA binding are the first steps in both processes, it should be possible to design a single material for both regulation and detection. To the best of our knowledge, however, a material capable of both mRNA regulation and detection has not been reported.<sup>39</sup> Such materials must be readily taken up by cells, stable in intracellular environments, capable of binding nucleic acids, and possess a switchable signal that can be conveniently detected.

Previous work by our group has demonstrated that oligonucleotide gold nanoparticle conjugates readily enter cells, and function as composite antisense nanoconjugates that outperform molecular antisense oligonucleotides in terms of stability and gene silencing ability.<sup>33</sup> Additionally, we have demonstrated that gold nanoparticles conjugated to short, fluorophore-labeled oligonucleotide duplexes act as intracellular nano-flares that provide a fluorescence signal that correlated with the presence and abundance of a specific intercellular nucleic acid and outperforms the uptake ability and stability of molecular beacons.<sup>34</sup> Based on these observations, we hypothesized that oligonucleotide gold nanoconjugates would be ideal ‘theranostic’ agents, combining intracellular gene regulation with detection. Herein, we characterize the target binding ability of these nanoconjugates, investigate their intracellular interaction with endogenous mRNA and demonstrate, for the first time, a single material capable of both regulating and detecting mRNA.

## RESULTS AND DISCUSSION

Nanoconjugates were designed with several features that make them well suited for both mRNA regulation and detection (Figure 1). The antisense oligonucleotide portion of the nanoconjugate targets an mRNA region selected to control expression of survivin,<sup>40</sup> a well-studied gene used in cancer diagnosis and treatment.<sup>41</sup> Additionally, the nanoconjugate recognition sequence is a DNA-LNA chimera, where the LNA bases serve to increase mRNA binding affinity, thereby increasing detection<sup>42</sup> and regulation efficiency.<sup>43, 44</sup> Finally, the nanoconjugate contains fluorophore-labeled ‘flare’ oligonucleotides that are designed to dissociate upon target binding. The bound ‘flare’ is quenched by the gold particle, so the dissociation can be detected as an increase fluorescence intensity.<sup>4</sup> This approach stands in contrast to previous studies where nanoconjugates were designed for either regulation or detection but not both.<sup>34, 45, 46</sup>

To prepare the nanoconjugates, citrate-capped gold nanoparticles were functionalized with thiol-terminated antisense oligonucleotides following literature procedures.<sup>47</sup> A high surface coverage ( $90 \pm 10$  oligonucleotides per nanoparticle) was achieved by slowly increasing the sodium chloride concentration to 0.3 M. These nanoconjugates were purified by centrifugation, and a short, complementary, Cy5-labeled oligonucleotide was added (Figure 1). A second nanoconjugate ( $86 \pm 4$  oligonucleotides per nanoparticle) that lacks the full antisense sequence was also synthesized to serve as a control.

To characterize this design, we first examined the response of the nanoconjugates (survivin and control) to synthetic DNA targets. This initial characterization is important when comparing cell populations that are treated with different nanoconjugates (*vide infra*). The nanoconjugate (1 nM) was added to a solution of phosphate buffered saline (pH 7.4), and the fluorescence of the solution was measured (Figure 2). In the absence of a target, both solutions of nanoconjugates exhibited a low fluorescence signal. The addition of the survivin target results in a 3.7 fold increase in the fluorescence associated with the survivin nanoconjugate. In the case of the control nanoconjugate, little response is observed. The sequence specific increase in fluorescence is consistent with ‘flare’ release from the gold nanoparticle surface.

In order to detect target mRNA it is critical for the nanoconjugates to respond to their target rapidly. In order to investigate the rate of flare release we added an excess of target to a solution containing the nanoconjugates and monitored the change in fluorescence over time. Fluorescence increases rapidly, reaching completion in approximately 10 minutes (Figure 2), which compares favorably to traditional nucleic acid probes such as molecular beacons.<sup>42, 48</sup>

We next designed experiments to characterize the specificity of the nanoconjugates for their complementary target. Nanoconjugates of an analogous design but containing a different

oligonucleotide sequence (see Methods Section) were challenged with a series of targets containing four, three, two or one base pair mismatches. Following incubation with these mismatch oligonucleotides, fluorescence was measured to examine nanoconjugate binding and subsequent flare release. Nanoconjugates that were treated with targets that contain four, three, or two mismatches show little increase in fluorescence signal, similar to nanoconjugates that were treated with buffer (Figure 3). Nanoconjugates that were treated with targets containing one mismatch show a fluorescence response. However, this signal is easily distinguished from that observed with the fully complementary target because it is 48% less intense. These results demonstrate that the nano-flares can be used to distinguish targets with a single base mismatch.

Having confirmed the specificity and selectivity of the nanoconjugates in an extracellular environment, we next studied their activity inside living cells. HeLa cells (a human cervical cancer line expressing survivin) were incubated with either survivin or control nanoconjugates (0.5 nM, see Methods Section). The cells were harvested and washed, and the cell-associated fluorescence was determined by flow cytometry. HeLa cells treated with survivin nanoconjugates are  $1.7 \pm 0.1$  times more fluorescent than cells treated with control nanoconjugates (Figure 4). Confocal fluorescence microscopy further confirmed that HeLa cells treated with survivin nanoconjugates have greater associated fluorescence than control nanoconjugates. When the experiments were repeated with C166 cells (a mouse cell line lacking a human survivin), both survivin and control nanoconjugates exhibited similar cell-associated fluorescence. Taken together, this series of experiments shows that the nanoconjugates can be used to distinguish different cell populations based on mRNA levels.

Next, we investigated the ability of these nanoconjugates to regulate intracellular mRNA levels. HeLa cell were incubated with survivin and control nanoconjugates (50, 5, or 0.5 nM) for 4 days. Following treatment, the cells were harvested, and the relative abundance of survivin mRNA was measured using real-time quantitative, reverse-transcription PCR (qRT-PCR). Survivin levels were normalized to actin mRNA, an off-target gene. Survivin mRNA levels were depleted by  $92\% \pm 4$  and  $80\% \pm 7$  when cells were treated with 50 and 5 nM survivin nanoconjugates, respectively (Figure 5). Survivin mRNA levels were not significantly changed when cells were treated with either a low concentration of survivin nanoconjugates (0.5 nM) or any concentration of control nanoconjugates. These data are consistent with a dose- and sequence-dependent reduction of mRNA. When compared to mRNA detection, gene regulation appears to require relatively high concentrations of nanoconjugate (5 rather than 0.5 nM) and relatively long exposure times (4 days rather than 6 hours). This agrees well with previous studies and is likely due to several factors including: cellular feedback loops that compensate for mRNA loss, efficient detection of mRNA when only a small percentage of the total mRNA population is bound, and rapid flare release followed by relatively slow mRNA degradation.<sup>24, 39, 45, 49, 50</sup>

The direct observation of reduced mRNA levels (Figure 5) can elucidate the mechanism of nanoconjugate gene regulation, which previously has only been investigated for traditional antisense oligonucleotides. In the case of molecular antisense, mRNA binding leads to enzyme activity which degrades the DNA/RNA hybrids. In the case of the nanoconjugates, we were interested in determining whether differences in target binding,<sup>23</sup> enzyme activity<sup>24</sup> and steric bulk between the nanoconjugate and traditional oligonucleotides would affect the mechanism of gene regulation. In previous work using similar nanoconjugates, we observed depletion in protein levels,<sup>45</sup> which can be caused by either translation inhibition or mRNA depletion.<sup>37</sup> Here, we find that nanoconjugates deplete mRNA, a phenomenon that has been observed with traditional antisense oligonucleotides. Our experiments indicate that this mechanism is important, not only for traditional antisense oligonucleotides, but also for nanoconjugates that function in gene regulation pathways.

## CONCLUSIONS

In summary, we have designed, synthesized, and characterized a nanoconjugate that can both detect and regulate intracellular mRNA levels. These nanoconjugates signal the presence of target mRNA with the release of a 'flare' sequence, which results in an increase in fluorescence. The target binding and response of the nano-flare is rapid and capable of recognizing single base-pair mismatches. The same nanoconjugates deplete mRNA levels by as much as  $92\% \pm 4$  in a dose- and sequence-dependent manner, consistent with enzymatic degradation of targeted mRNA. Although similar gene regulation and detection strategies have been used in this past, this work represents the first combination of gene regulation and detection in a single material. Moreover, we show for the first time that oligonucleotide functionalized particles directly deplete mRNA levels. These nanomaterials are a promising first step towards the development of mRNA directed 'theranostics' and are expected to combine the advantages of gene therapy with personalized medicine.

## METHODS

### Oligonucleotide synthesis

Oligonucleotides were synthesized with an Expedite 8909 Nucleotide Synthesis System (ABI) using standard solid-phase phosphoramidite methodology. The bases and reagents were purchased from Glen Research. All oligonucleotides were purified by reverse-phase high performance liquid chromatography (HPLC). The oligonucleotide sequences used in this study are shown below. The underlined nucleotides are LNA, all others are DNA. Target DNA: 5' - CAA GGA GCT GGA AGG CTG GG - 3', Survivin: 5' - CCC AGC CTT CCA GCT CCT TG - (A)<sub>10</sub> - propylthiol - 3', Control: 5' - TCT CCC CAG CCA GCT CCT TG - (A)<sub>10</sub> - propylthiol - 3', Flare: 5' - (Cy5) - TCA AGG AGC TGG - 3'. Particle used in selectivity experiments: 5' - GCT TGC TTT GTG ATC ATA CC (A)<sub>10</sub> - propylthiol - 3'; Full complement: 5' - GGT ATG ATC ACA AAG CAA GC - 3'; Single mismatch: 5' - GGT ATC ATC ACA AAG CAA GC - 3'; two mismatch: GGT ATC ATC ACA AAG GAA GC - 3'; three mismatch: 5' - GGT ATC ATC AGA AAG GAA GC - 3'; four mismatch: 5' - GCT ATC ATC AGA AAG GAA GC - 3'.

### Oligonucleotide gold nanoparticle conjugates

Alkyl-thiol-modified oligonucleotides (final concentration = 2  $\mu$ M) were added to a 10 nM solution of  $13 \pm 1$  nm gold NPs. After 2 hours, sodium dodecylsulphate (SDS), phosphate buffer (pH = 7.4), and sodium chloride were added to achieve final concentrations of 0.1 %, 10 mM, and 0.1 M, respectively. An additional aliquot of sodium chloride was added to achieve a final concentration of 0.3 M, and the mixture was shaken overnight. The functionalized nanoparticles were purified from unreacted materials by three successive rounds of centrifugation (16,000 rcf, 20 min), supernatant removal, and resuspension in phosphate buffered saline (PBS) (137 mM NaCl, 10 mM phosphate, 2.7mM KCl, pH 7.4, Hyclone).

### Oligonucleotide loading

The concentrations of the purified nanoconjugates were determined by UV/vis spectrophotometry ( $\lambda = 524$ ,  $\epsilon = 2.7 \times 10^8 \text{ L} \cdot \text{mol}^{-1} \cdot \text{cm}^{-1}$ ). The nanoconjugates were then treated with KCN solution (0.1 M) to oxidatively dissolve the gold particles and liberate the surface-coordinated oligonucleotides. Oligonucleotide concentration was determined using a commercially available kit (Oligreen; Invitrogen) following the manufacturer's recommendations. The average number of oligonucleotides conjugated to a nanoparticle was calculated by dividing the concentration of oligonucleotides by the concentration of nanoparticles.

### **'Flare' duplex formation**

Purified nanoconjugates (100 nM) and Cy5-labeled 'flare' DNA (1 mM) were combined in PBS. The mixture was heated to 70°C and slowly cooled to room temperature over 4 hours to allow hybridization. The nanoconjugates were sterilized using a 0.2 µm acetate syringe filter (GE Healthcare) and stored at 4°C.

### **Fluorescence spectroscopy**

Fluorescence measurements were recorded on a Jobin Yvon Fluorolog FL3-22 exciting at 633 nm and measuring emission from 650 to 750 nm in 1 nm increments. Static fluorescence was measured on samples containing nanoconjugates (1 nM) in PBS with 0.1 % Tween-20 (Sigma). The complementary target (200 nM) was added and the solutions were remeasured. The time course experiment was carried out by treating solutions of nanoconjugates with target and measuring fluorescence (670 nm) in 20-second increments for 1 hour.

### **Cell culture**

HeLa (human cervical cancer) and C166 (mouse endothelial) cells were obtained from the American Tissue Culture Collection (ATCC) and were grown in Essential Minimum Eagles Medium (EMEM) and Dulbecco's modified Eagles medium (DMEM), respectively. Both media contained 10 % heat inactivated fetal bovine serum, and the cells were maintained at 37°C in 5% CO<sub>2</sub>. Cells were seeded 1 day prior to treatment with the nanoconjugates.

### **Flow cytometry**

Cells were treated with media containing nanoconjugates (0.5 nM) for 6 hours, the media was replaced, and the cells were incubated for an additional 18 hours. The next day, cells were washed with PBS, detached from the growth surface using the enzyme trypsin, and collected. Flow cytometry was performed using a DakoCytomation CyAn, exciting at 635 nm. The data reported in Figure 3 represents the average cell associated fluorescence for a population of cells. The standard deviation for this data was calculated by comparing the values among 3 independent experiments. To normalize for cell-type, the values were reported as a fraction of the control nanoconjugate-treated cells.

### **Imaging**

Cells were grown on glass bottom wells to 20% confluence. Nanoconjugates (5 nM) were added, and the cells were treated in the same manner as described in the flow cytometry procedure. The cells were visualized with a Zeiss 510 LSM at 63x magnification using a 633 nm HeNe laser excitation source.

### **RT-PCR**

Cells were treated with nanoconjugates (0.5, 5, and 50 nM) for 4 days, as described above. The cells were harvested, and total RNA was extracted using phenol, guanidine isothiocyanate and chloroform (TRIzol reagent, Invitrogen) followed by treatment with DNase according to the manufacturer's protocol. This procedure is commonly used in antisense experiments because it disrupts the antisense oligonucleotide-RNA duplex,<sup>51</sup> allowing purification of mRNA and preventing interference by the antisense oligonucleotides at later steps.<sup>40, 52</sup> RNA (5 µg) was reverse transcribed using Superscript III (Invitrogen). PCR was performed on cDNA with SYBR Green dye on a Stratagene Mx3000P System. The relative abundance of each mRNA transcript was normalized to actin expression and compared to untreated cells to determine the increased expression. The standard deviation for this data was calculated from 3 independent experiments. The primers used to make cDNA in this experiment were: survivin forward, 5' - ATG GGT GCC CCG ACG TTG - 3'; survivin reverse, 5' - AGA GGC CTC AAT CCA TGG

- 3'; actin forward, 5' - ATC ATT GCT CCA CCA GAA CG - 3'; actin reverse, 5' - AAG GTA GAT AGA GAA GCC AAG - 3'.

## Acknowledgement

C. Mirkin acknowledges a Cancer Center for Nanotechnology Excellence (NCI-CCNE) award for support of this research. C. Mirkin is also grateful for an NIH Director's Pioneer Award. D. Seferos was supported by the LUNgevity Foundation-American Cancer Society Postdoctoral Fellowship in Lung Cancer.

## REFERENCES

1. Cerruti MG, Sauthier M, Leonard D, Liu D, Duscher G, Feldheim DL, Franzen S. Gold and silica-coated gold nanoparticles as thermographic labels for DNA detection. *Anal. Chem* 2006;78:3282–3288. [PubMed: 16689528]
2. Du H, Disney MD, Miller BL, Krauss TD. Hybridization-based unquenching of DNA hairpins on Au surfaces: Prototypical “molecular beacon” biosensors. *J. Am. Chem. Soc* 2003;125:4012–4013. [PubMed: 12670198]
3. Du H, Strohsahl CM, Camera J, Miller BL, Krauss TD. Sensitivity and specificity of metal surface-immobilized “molecular beacon” biosensors. *J. Am. Chem. Soc* 2005;127:7932–7940. [PubMed: 15913384]
4. Dubertret B, Calame M, Libchaber AJ. Single-mismatch detection using gold-quenched fluorescent oligonucleotides. *Nat. Biotechnol* 2001;19:365–370. [PubMed: 11283596]
5. Faulds K, Fruk L, Robson DC, Thompson DG, Enright A, Smith WE, Graham D. A new approach for DNA detection by SERRS. *Faraday Discuss* 2006;132:261–268. [PubMed: 16833121]
6. Graham D, Faulds K, Smith WE. Biosensing using silver nanoparticles and surface enhanced resonance Raman scattering. *Chem. Commun. Cambridge, U.K* 2006;42:4363–4371.
7. He L, Musick MD, Nicewarner SR, Salinas FG, Benkovic SJ, Natan MJ, Keating CD. Colloidal Au-enhanced surface plasmon resonance for ultrasensitive detection of DNA hybridization. *J. Am. Chem. Soc* 2000;122:9071–9077.
8. Liu XJ, Farmerie W, Schuster S, Tan WH. Molecular beacons for DNA biosensors with micrometer to submicrometer dimensions. *Anal. Biochem* 2000;283:56–63. [PubMed: 10929808]
9. Medintz IL, Berti L, Pons T, Grimes AF, English DS, Alessandrini A, Facci P, Mattoussi H. A reactive peptidic linker for self-assembling hybrid quantum dot-DNA bioconjugates. *Nano Lett* 2007;7:1741–1748. [PubMed: 17530814]
10. Stoermer RL, Keating CD. Distance-dependent emission from dye-labeled oligonucleotides on striped Au/Ag nanowires: Effect of secondary structure and hybridization efficiency. *J. Am. Chem. Soc* 2006;128:13243–13254. [PubMed: 17017805]
11. Yao G, Wang L, Wu YR, Smith J, Xu JS, Zhao WJ, Lee EJ, Tan WH. FloDots: luminescent nanoparticles. *Anal. Bioanal. Chem* 2006;385:518–524. [PubMed: 16715275]
12. Sandhu KK, McIntosh CM, Simard JM, Smith SW, Rotello VM. Gold nanoparticle-mediated Transfection of mammalian cells. *Bioconjugate Chem* 2002;13:3–6.
13. Yang RH, Jin JY, Chen Y, Shao N, Kang HZ, Xiao Z, Tang ZW, Wu YR, Zhu Z, Tan WH. Carbon nanotube-quenched fluorescent oligonucleotides: Probes that fluoresce upon hybridization. *J. Am. Chem. Soc* 2008;130:8351–8358. [PubMed: 18528999]
14. Alivisatos AP, Johnsson KP, Peng XG, Wilson TE, Loweth CJ, Bruchez MP, Schultz PG. Organization of ‘nanocrystal molecules’ using DNA. *Nature* 1996;382:609–611. [PubMed: 8757130]
15. Reinhard BM, Sheikholeslami S, Mastroianni A, Alivisatos AP, Liphardt J. Use of plasmon coupling to reveal the dynamics of DNA bending and cleavage by single EcoRV restriction enzymes. *Proc. Natl. Acad. Sci. U.S.A* 2007;104:2667–2672. [PubMed: 17307879]
16. Sonnichsen C, Reinhard BM, Liphardt J, Alivisatos AP. A molecular ruler based on plasmon coupling of single gold and silver nanoparticles. *Nat. Biotechnol* 2005;23:741–745. [PubMed: 15908940]



17. Zheng JW, Constantinou PE, Micheel C, Alivisatos AP, Kiehl RA, Seeman NC. Two-dimensional nanoparticle arrays show the organizational power of robust DNA motifs. *Nano Lett* 2006;6:1502–1504. [PubMed: 16834438]
18. Wu YR, Phillips JA, Liu HP, Yang RH, Tan WH. Carbon Nanotubes Protect DNA Strands during Cellular Delivery. *ACS Nano* 2008;2:2023–2028. [PubMed: 19206447]
19. Gao XH, Yang LL, Petros JA, Marshal FF, Simons JW, Nie SM. In vivo molecular and cellular imaging with quantum dots. *Curr. Opin. Biotechnol* 2005;16:63–72. [PubMed: 15722017]
20. Maxwell DJ, Taylor JR, Nie SM. Self-assembled nanoparticle probes for recognition and detection of biomolecules. *J. Am. Chem. Soc* 2002;124:9606–9612. [PubMed: 12167056]
21. Dulkeith E, Ringler M, Klar TA, Feldmann J, Javier AM, Parak WJ. Gold nanoparticles quench fluorescence by phase induced radiative rate suppression. *Nano Lett* 2005;5:585–589. [PubMed: 15826091]
22. Storhoff JJ, Lazarides AA, Mucic RC, Mirkin CA, Letsinger RL, Schatz GC. What controls the optical properties of DNA-linked gold nanoparticle assemblies? *J. Am. Chem. Soc* 2000;122:4640–4650.
23. Lytton-Jean AKR, Mirkin CA. A thermodynamic investigation into the binding properties of DNA functionalized gold nanoparticle probes and molecular fluorophore probes. *J. Am. Chem. Soc* 2005;127:12754–12755. [PubMed: 16159241]
24. Seferos DS, Prigodich AE, Giljohann DA, Patel PC, Mirkin CA. Polyvalent DNA Nanoparticle Conjugates Stabilize Nucleic Acids. *Nano Lett* 2009;9:308–311. [PubMed: 19099465]
25. Giljohann DA, Seferos DS, Patel PC, Millstone JE, Rosi NL, Mirkin CA. Oligonucleotide loading determines cellular uptake of DNA-modified gold nanoparticles. *Nano Lett* 2007;7:3818–3821. [PubMed: 17997588]
26. Mirkin CA, Letsinger RL, Mucic RC, Storhoff JJ. A DNA-based method for rationally assembling nanoparticles into macroscopic materials. *Nature* 1996;382:607–609. [PubMed: 8757129]
27. Park SY, Lytton-Jean AKR, Lee B, Weigand S, Schatz GC, Mirkin CA. DNA-programmable nanoparticle crystallization. *Nature* 2008;451:553–556. [PubMed: 18235497]
28. Shyr MHS, Wernette DP, Wiltzius P, Lu Y, Braun PV. DNA and DNAzyme-Mediated 2D colloidal assembly. *J. Am. Chem. Soc* 2008;130:8234–8240. [PubMed: 18540602]
29. Taton TA, Mirkin CA, Letsinger RL. Scanometric DNA array detection with nanoparticle probes. *Science* 2000;289:1757–1760. [PubMed: 10976070]
30. Liu JW, Lu Y. Non-base pairing DNA provides a new dimension for controlling aptamer-linked nanoparticles and sensors. *J. Am. Chem. Soc* 2007;129:8634–8643. [PubMed: 17567134]
31. Nam JM, Thaxton CS, Mirkin CA. Nanoparticle-based bio-bar codes for the ultrasensitive detection of proteins. *Science* 2003;301:1884–1886. [PubMed: 14512622]
32. Elghanian R, Storhoff JJ, Mucic RC, Letsinger RL, Mirkin CA. Selective colorimetric detection of polynucleotides based on the distance-dependent optical properties of gold nanoparticles. *Science* 1997;277:1078–1081. [PubMed: 9262471]
33. Rosi NL, Giljohann DA, Thaxton CS, Lytton-Jean AKR, Han MS, Mirkin CA. Oligonucleotide-modified gold nanoparticles for intracellular gene regulation. *Science* 2006;312:1027–1030. [PubMed: 16709779]
34. Seferos DS, Giljohann DA, Hill HD, Prigodich AE, Mirkin CA. Nano-flares: Probes for transfection and mRNA detection in living cells. *J. Am. Chem. Soc* 2007;129:15477–15479. [PubMed: 18034495]
35. Agbasi-Porter C, Ryman-Rasmussen J, Franzen S, Feldheim D. Transcription inhibition using oligonucleotide-modified gold nanoparticles. *Bioconjugate Chem* 2006;17:1178–1183.
36. Ozdemir V, Williams-Jones B, Glatt SJ, Tsuang MT, Lohr JB, Reist C. Shifting emphasis from pharmacogenomics to theragnostics. *Nat. Biotechnol* 2006;24:942–947. [PubMed: 16900136]
37. Crooke ST. Progress in antisense technology. *Annu. Rev. Med* 2004;55:61–95. [PubMed: 14746510]
38. Wang K, Tang Z, Yang CJ, Kim Y, Fang X, Li W, Wu Y, Medley CD, Cao Z, Li J, Colon P, Lin H, Tan W. Molecular Engineering of DNA: Molecular Beacons. *Angew. Chem., Int. Ed* 2009;48:856–870.
39. Peng XH, Cao ZH, Xia JT, Carlson GW, Lewis MM, Wood WC, Yang L. Real-time detection of gene expression in cancer cells using molecular beacon imaging: New strategies for cancer research. *Cancer Res* 2005;65:1909–1917. [PubMed: 15753390]

40. Olie RA, Simoes-Wust AP, Baumann B, Leech SH, Fabbro D, Stahel RA, Zangemeister-Wittke U. A novel antisense oligonucleotide targeting survivin expression induces apoptosis and sensitizes lung cancer cells to chemotherapy. *Cancer Res* 2000;60:2805–2809. [PubMed: 10850418]
41. Altieri DC. Survivin, cancer networks and pathway-directed drug discovery. *Nat. Rev. Cancer* 2008;8:61–70. [PubMed: 18075512]
42. Wang L, Yang CYJ, Medley CD, Benner SA, Tan WH. Locked nucleic acid molecular beacons. *J. Am. Chem. Soc* 2005;127:15664–15665. [PubMed: 16277483]
43. Kaur H, Babu BR, Maiti S. Perspectives on chemistry and therapeutic applications of Locked Nucleic Acid LNA. *Chem. Rev. Washington, DC, U.S* 2007;107:4672–4697.
44. Kurreck J, Wyszko E, Gillen C, Erdmann VA. Design of antisense oligonucleotides stabilized by locked nucleic acids. *Nucleic Acids Res* 2002;30:1911–1918. [PubMed: 11972327]
45. Seferos DS, Giljohann DA, Rosi NL, Mirkin CA. Locked nucleic acid-nanoparticle conjugates. *ChemBioChem* 2007;8:1230–1232. [PubMed: 17562553]
46. Patel PC, Giljohann DA, Seferos DS, Mirkin CA. Peptide antisense nanoparticles. *Proc. Natl. Acad. Sci. U.S.A* 2008;105:17222–17226. [PubMed: 19004812]
47. Storhoff JJ, Elghanian R, Mucic RC, Mirkin CA, Letsinger RL. One-pot colorimetric differentiation of polynucleotides with single base imperfections using gold nanoparticle probes. *J. Am. Chem. Soc* 1998;120:1959–1964.
48. Tyagi S, Kramer FR. Molecular beacons: Probes that fluoresce upon hybridization. *Nat. Biotechnol* 1996;14:303–308. [PubMed: 9630890]
49. Lennox KA, Sabel JL, Johnson MJ, Moreira BG, Fletcher CA, Rose SD, Behlke MA, Laikhter AL, Walder JA, Dagle JM. Characterization of modified antisense oligonucleotides in *Xenopus laevis* embryos. *Oligonucleotides* 2006;16:26–42. [PubMed: 16584293]
50. Perlette J, Tan WH. Real-time monitoring of intracellular mRNA hybridization inside single living cells. *Anal. Chem* 2001;73:5544–5550. [PubMed: 11816586]
51. Goda SK, Minton NP. A Simple Procedure for Gel-Electrophoresis and Northern Blotting of Rna. *Nucleic Acids Res* 1995;23:3357–3358. [PubMed: 7545288]
52. Rekasi Z, Horvath RA, Klausz B, Nagy E, Toller GL. Suppression of serotonin N-acetyltransferase transcription and melatonin secretion from chicken pinealocytes transfected with Bmal1 antisense oligonucleotides containing locked nucleic acid in superfusion system. *Mol. Cell. Endocrinol* 2006;249:84–91. [PubMed: 16517056]



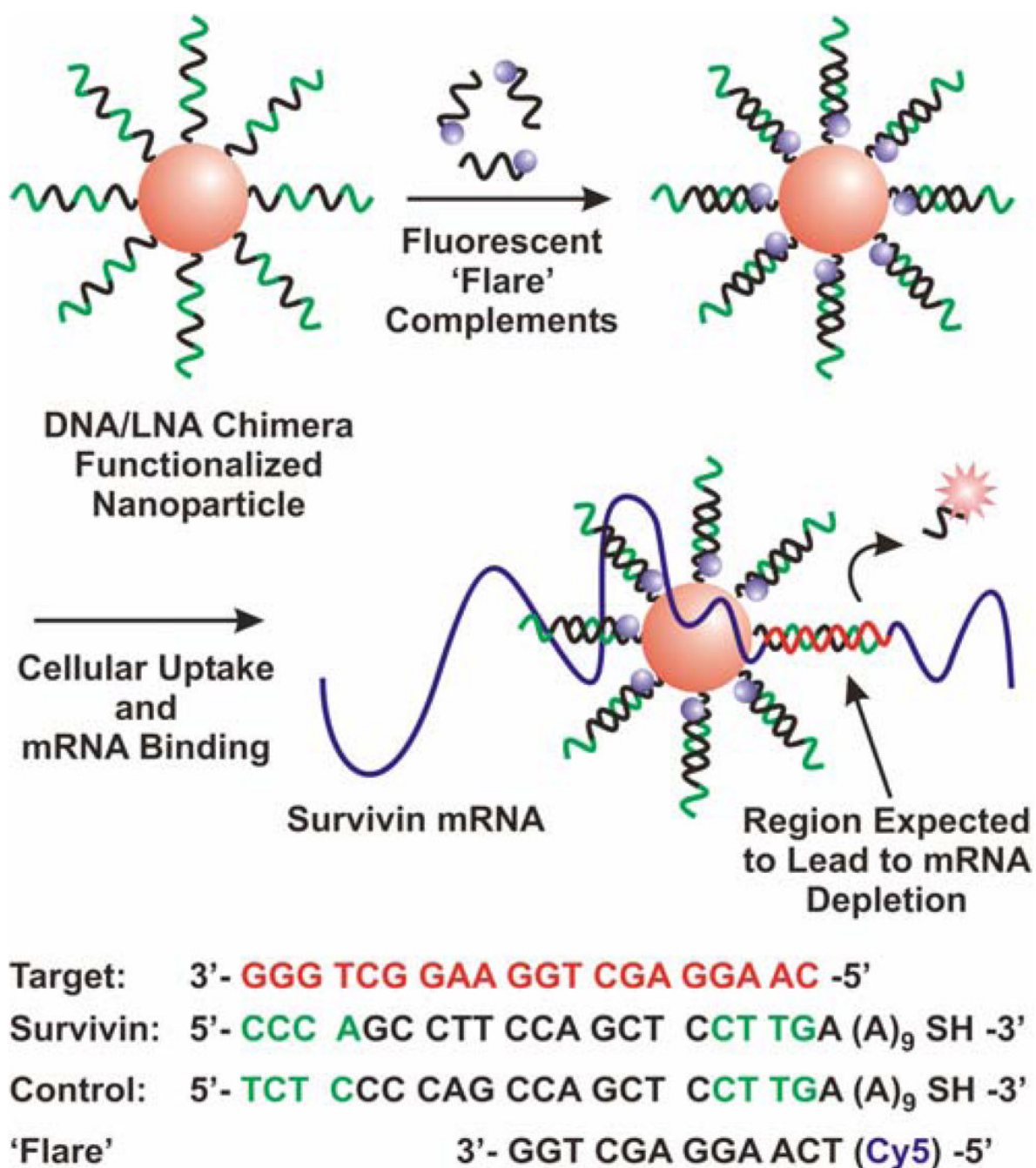


**Figure 1.** mRNA depletion and detection using survivin nanoconjugates (13 nm gold particle shown in orange). DNA is shown in black, LNA in green. mRNA is shown in purple, while the target region of the mRNA is shown in red. Cy5 is shown in purple or pink when quenched or released, respectively.

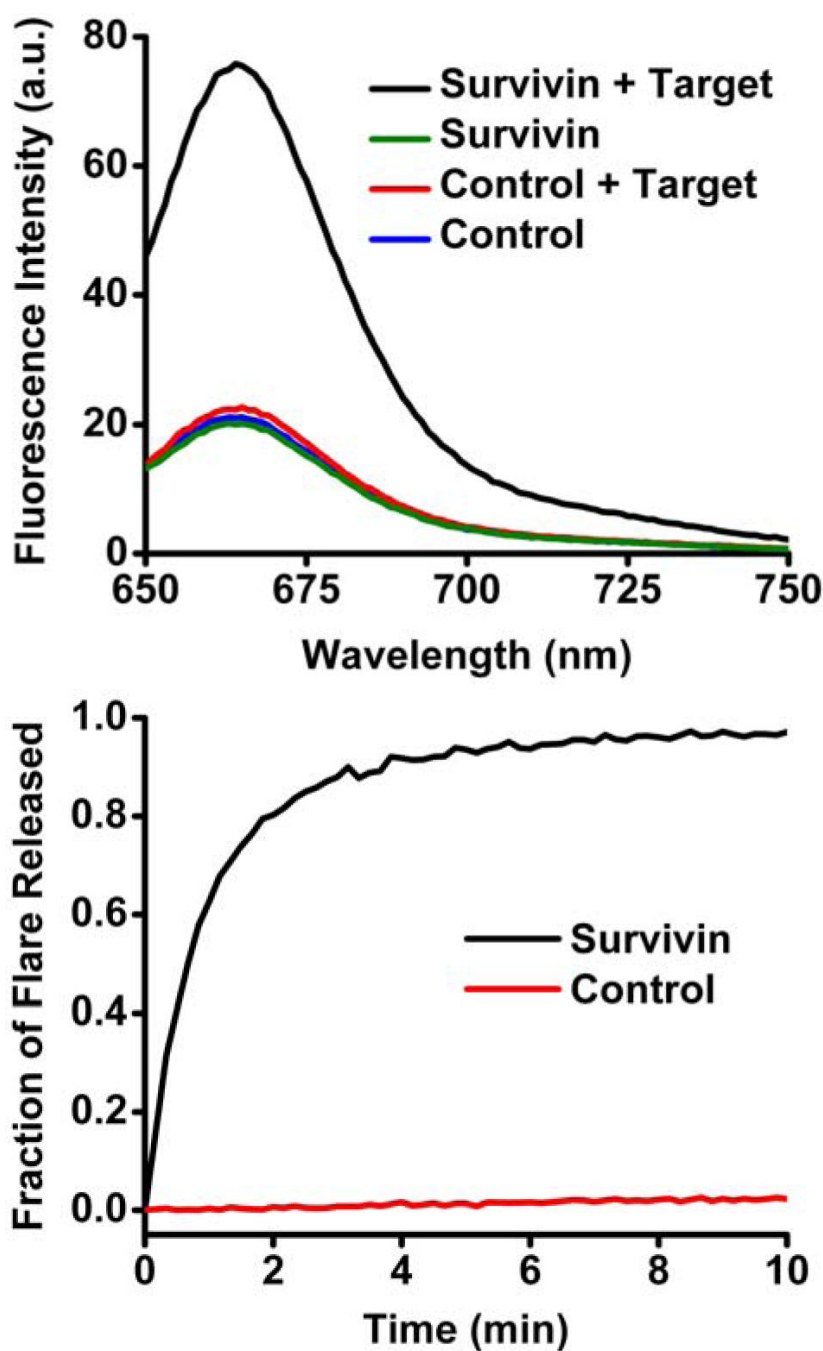


**Figure 2.**

Survivin nanoconjugates respond to synthetic target DNA. Top: fluorescence spectra of nanoconjugates before and after addition of target DNA. Bottom: time course of fluorescence measured associated with flare release. Target DNA is added at time zero. Complete release was determined by saturating the nanoparticle with excess target DNA.

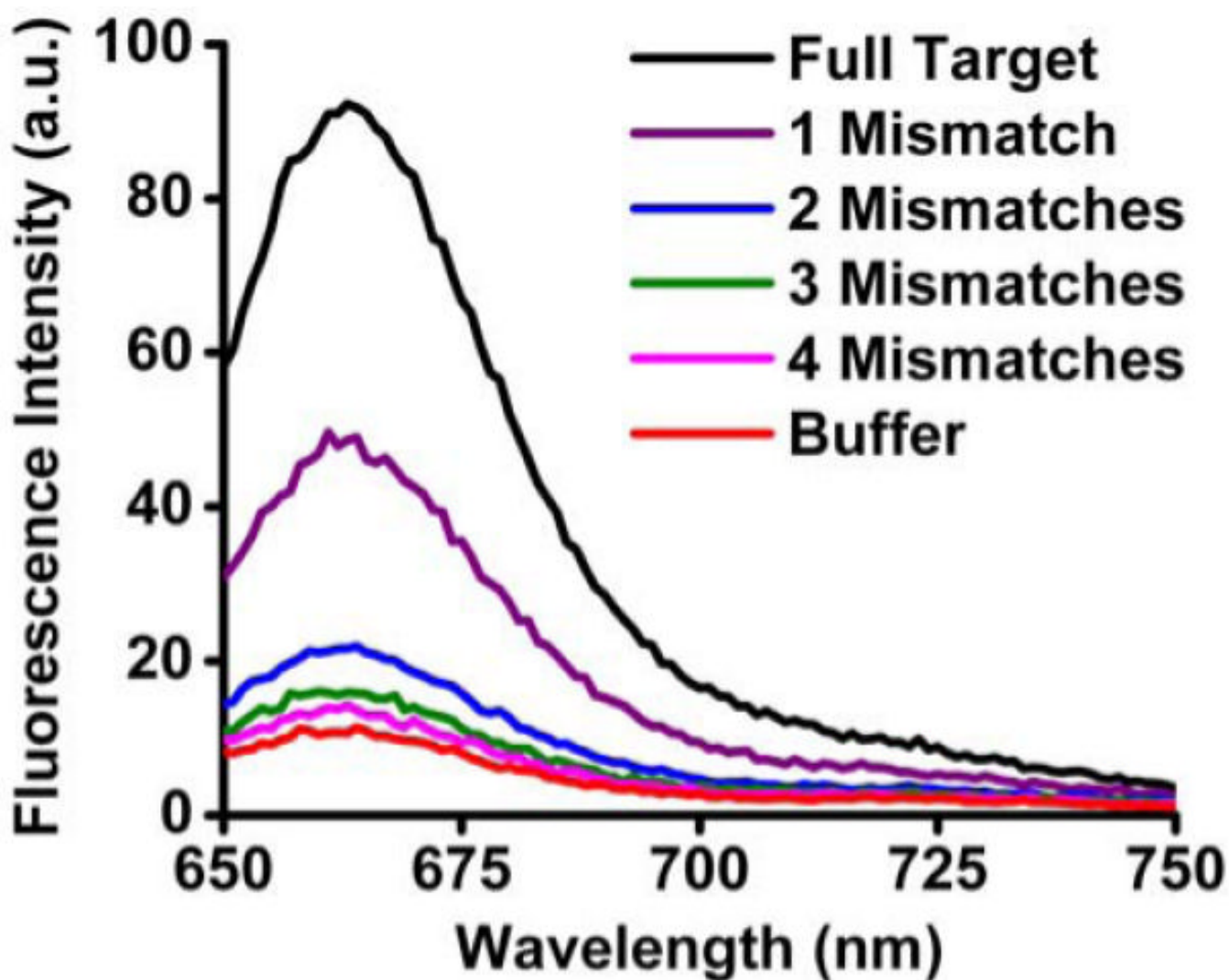


**Figure 3.** Nanoconjugates distinguish mismatched nucleic acids. Fluorescence spectra of nanoconjugates challenged with buffer (no target), complementary target and those containing 1, 2, 3, or 4 mismatches.

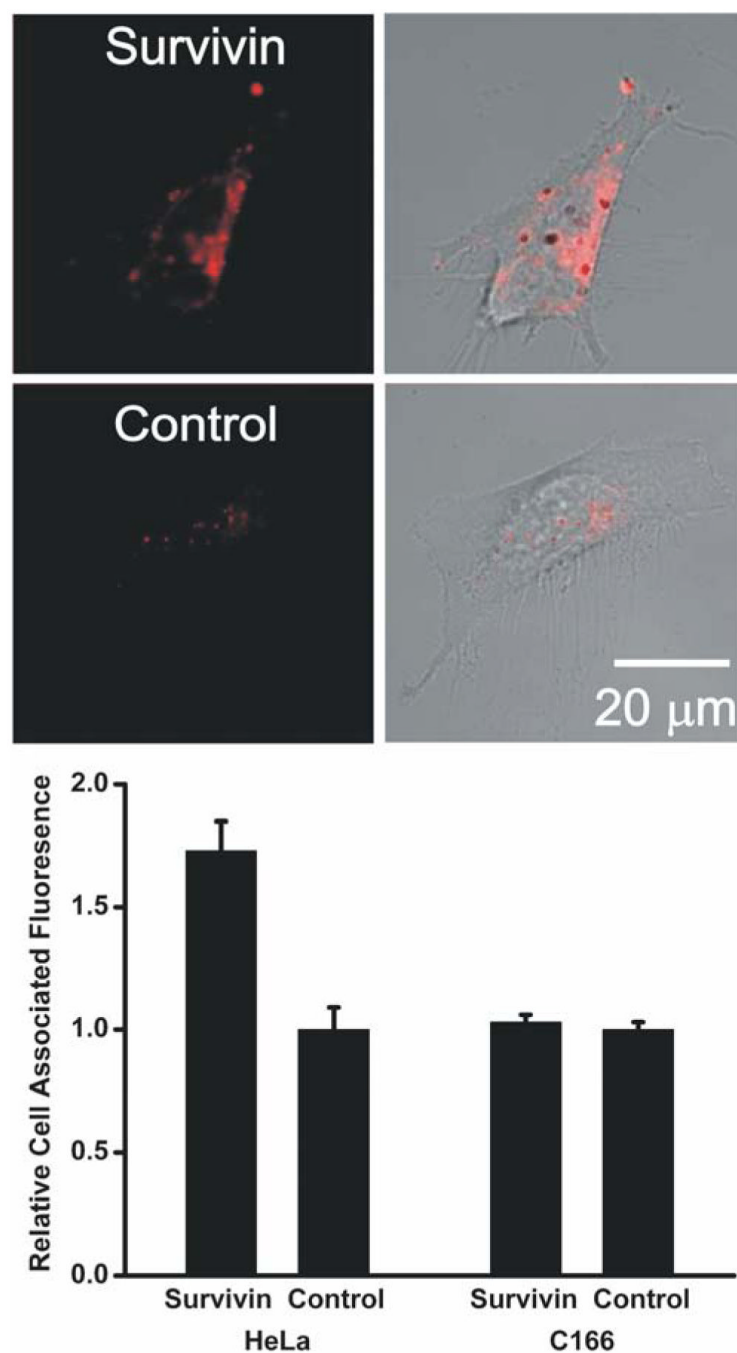


**Figure 4.**

Survivin nanoconjugates respond to intracellular mRNA. Top, confocal fluorescence microscopy of HeLa cells treated with either survivin or control nanoconjugates. Cy5 fluorescence (red) associated with 'flare' and bright field images (see Figure 1). Bottom, flow cytometry data for HeLa and C166 cells treated with both nanoconjugates. The fluorescence was normalized to the cell population treated with control nanoparticles.

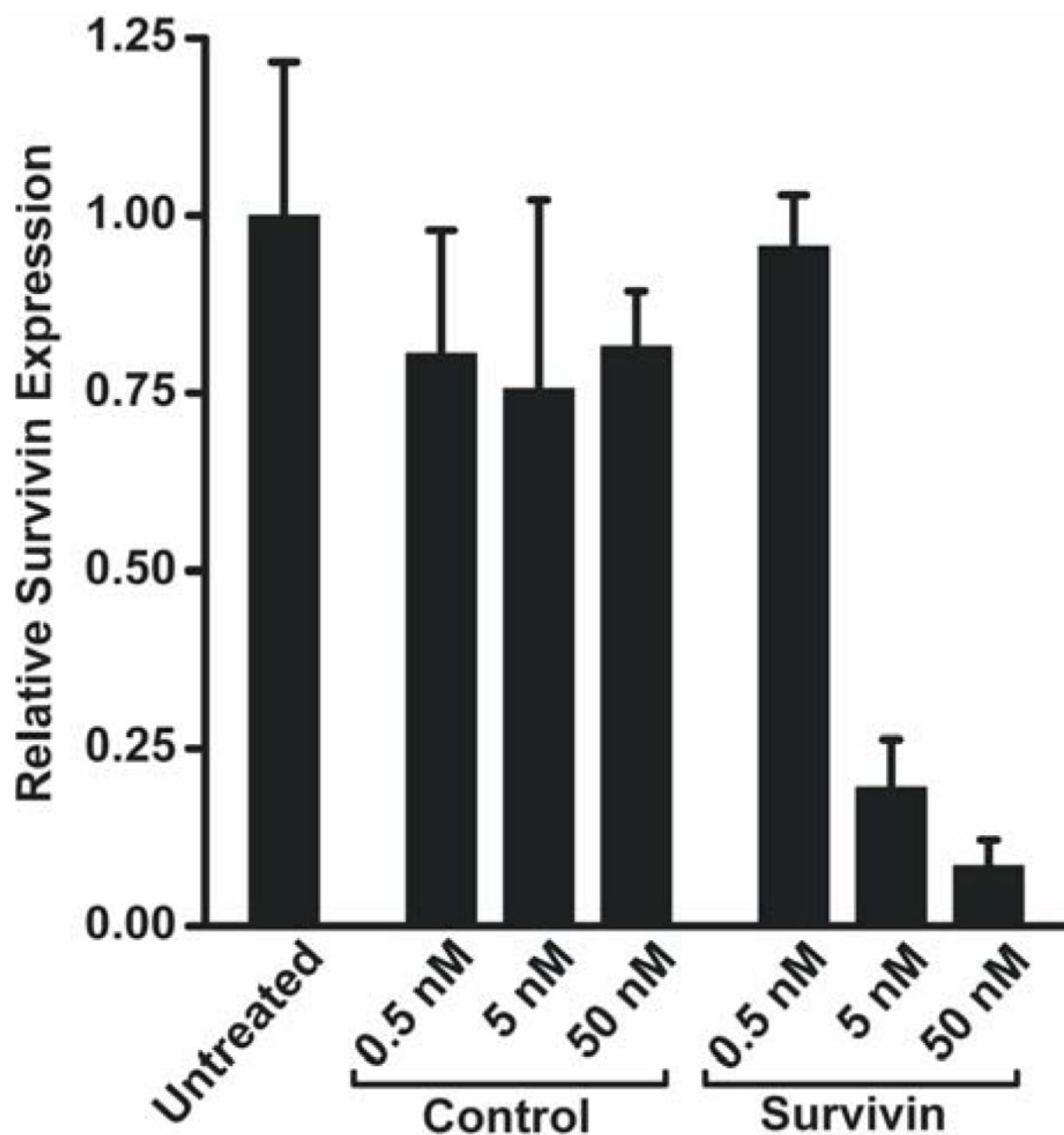


**Figure 5.**

The effect of nanoconjugates on survivin mRNA levels in HeLa cells. The relative abundance of survivin mRNA was determined by RT-PCR and normalized to expression levels in untreated cells.